AIAA JOURNAL
Vol. 37, No. 10, October 1999

# Supersonic Expelled Jets from Squeezed Fluid Singularities

M. J. Gagen*
*University of Queensland, Brisbane, Queensland 4072, Australia*

**It is demonstrated analytically and experimentally that supersonic flows can be achieved using hand-powered tabletop apparatus designed to exploit singularities in fluid dynamic equations. Squeezed fluids occupy volumes that are shrinking in time because of external applied forces with boundaries closing to zero separation in the limit. Fluid velocity gradients are inversely proportional to the shrinking spatial separations, and closure to zero sends these gradients to infinity. These infinite gradients can then drive energetic fluid expulsion in perpendicular nonsqueezed directions. Mathematically, squeezing introduces regular singular points into the governing fluid equations to force singular solutions.**

## I. Introduction

FLUID dynamics research has long sought to understand and manipulate the gradient singularities called shock waves where finite discontinuities appear in fluid densities and velocities.[1,2] Similarly, pistonlike systems that squeeze fluids are exploited to generate potential singularities in density and other fluid parameters of interest. For instance, shock tunnels compress gases to the point where they burst thick metal diaphragms,[2,3] the handheld Diamond-Anvil generates up to $2 \times 10^6$ atmospheres of pressure,[4] cavitation produces energy densities sufficient to pit steel,[5] sonoluminescence generates temperatures in excess of 100,000 deg,[6–8] explosive compression of magnetic fields gives planned strengths of 1000 T (Refs. 9 and 10), whereas experiments on supernovae collapse use inertial confinement fusion to obtain temperatures in excess of $100 \times 10^6$ deg.[11]

Of more interest to this paper are flow systems designed to generate velocity singularities. Examples include the separation point of boundary layers[1,2] where both fluid parameters and fluid gradients develop singularities and where respectively, analytic solutions, the continuum assumptions of fluid mechanics, and most simulation approaches all break down. In addition, high-Reynolds-numberhydrodynamic flows have been shown to develop singular velocity derivatives in finite time.[12]

The preceding approaches feature fluid flow in regions characterized by stationary boundaries. In contrast, we consider regions with moving boundaries chosen so that the boundary equations of motion radically change the nature of the solutions to the fluid equations. In effect, the boundary dynamics modifies the underlying system of fluid equations to change the available solution space. An example of a system that uses dynamical boundaries to access velocity singularities is the partitioning of a fluid into two parts as, for instance, when a fluid drop fissions in two[13,14] or as thin films are pinched to zero thickness.[15] A speculative proposal to accelerate interstellar spacecraft using this same velocity singularity created as two asteroids collide or scissor together has also been made.[16]

This paper generalizes Ref. 15 to large-scale systems by imposing external squeezing forces on simple fluid systems to obtain velocity singularities and supersonic expelled jets. We demonstrate analytically, numerically, and experimentally that simple hand-powered equipment can drive supersonic flows at potentially very high Mach numbers.

This result is counterintuitive as previous fluid dynamical models generally restrict their attention to stationary and nonsqueezed boundaries. (A rare counterexample considers high-speed trains entering tunnels.[17,18]) Further, the computational intractability of simulating a fluid singularity (an infinite amount of computer resources are required) has led to singularity problems being generally ignored. In contrast, we consider that the pistonlike systems just mentioned can have their designs modified so that their fluid singularities are harnessed to drive supersonic escape flows. Then, the same squeezing singularities that provide elegant access to extreme fluid temperatures and densities will also provide simple and elegant mechanisms to drive escape flows at high Mach values. The research question of interest is not whether these velocity singularities exist but is rather "How fast can we go?"

The ultimate answer to this question can only be obtained by considering regular singular points in relativistic fluid equations applied to large astrophysical systems. Elsewhere, we consider relativistic jets from astrophysical systems with immense crushing (or squeezing) gravitational fields.[19] At the other end of the scale, we also consider how the squeezing of car tire cavities contributes to the as yet unexplained far-field sound intensity of car tires.[20]

Singular solutions to fluid equations are forced when a regular singular point appears in the governing equations and is demonstrated in Sec. II using several well-known examples such as the cracking whip and one-dimensional fluid flow through pipes of variable cross section. We begin our analysis of squeezed systems by rederiving the Euler equations under squeezed boundary conditions in Sec. III. Subsequently, we discuss approximate analytic solutions to the squeezed Euler equations in Sec. IV and show numerical simulations of the expelled flows in Sec. V. Finally, in Sec. VI we show the results of an initial proof-of-concept experiment to confirm our earlier analysis.

## II. Velocity Singularities in Squeezed Fluids

Squeezed fluids occupy shrinking regions with boundaries closing to zero separation in the limit. Fluid velocity gradients are inversely proportional to the shrinking spatial separations, and closure to zero sends these gradients to infinity. The infinite gradients between the inside compressed region and the outside uncompressed region can then drive energetic fluid expulsion in directions perpendicular to the squeezing direction. This mechanism can be formalized using the continuity equation[1,2]

$$\partial_t \rho + \partial_x(\rho v_x) + \partial_y(\rho v_y) = 0 \tag{1}$$

proscribing fluid density $\rho$ with velocities $(v_x, v_y)$ in directions $(x, y)$. ($\partial_\alpha$ expresses rates of change in coordinate $\alpha$.) Consider a piston closing vertically in the $y$ direction with finite velocity differentials $\Delta(\rho v_y) < 0$ appearing over shrinking displacements $\Delta y \to 0$. A fully enclosed piston lacks escape flows ($v_x = 0$), giving

$$\partial_t \rho = -\frac{\Delta(\rho v_y)}{\Delta y} \to \infty \tag{2}$$

with singular solution $\rho(t) \to \infty$ in the limit $\Delta y \to 0$.

In contrast, consider a squeezed system that lacks constraining side walls so that escape flows are possible with $v_x \neq 0$. Such systems are then described by the modified continuity equation

$$\partial_t \rho + \partial_x(\rho v_x) = -\frac{\Delta(\rho v_y)}{\Delta y} \to \infty \tag{3}$$

Received 7 July 1998; revision received 29 January 1999; accepted for publication 15 March 1999. 

*Research Officer, Department of Physics; gagen@physics.uq.edu.au.

with singular solution $\rho(t) \to \infty$ and/or $v_x(t) \to \infty$ in the limit $\Delta y \to 0$. This equation models high-speed jets expelled perpendicular to applied squeezing forces.

As an example consider the cracking whip that transmits constant power (the fluid) through a medium of decreasing linear density. The constant rate of power flow is given by the product of the squared amplitude of wave motion and the density per unit length. Then, the tapering of the whip to zero density necessarily increases the amplitude until the tip speed breaks the sound barrier.[21,22] This velocity singularity appears in the governing equations giving the transverse displacement $\psi$ for a cracking whip under constant tension $T$, as

$$\rho(x)\partial_{tt}\psi = T\partial_{xx}\psi \tag{4}$$

The decrease in linear density $\rho(x) \to 0$ for large $x$ ensures that the transverse acceleration $\partial_{tt}\psi \to \infty$ to maintain the nonzero value of the right-hand side (RHS) of this equation.

A similar zero asymptote governs one-dimensional fluid flow through pipes of variable cross section. Here, conservation of mass ensures that the product of pipe area and fluid velocity remains a constant,[1,2] so that shrinking the pipe forces higher flow speeds. The governing equations relate linear density $\rho$ and horizontal velocity $v$ to cross-sectional area $A(x)$ via

$$\partial_t(\rho A) + \partial_x(\rho A v) = 0 \tag{5}$$

The injection form of this equation clarifies physical meaning in the limit of shrinking cross-sectional area $A \to 0$:

$$\partial_t(\rho) + \partial_x(\rho v) = -\frac{\rho v A'}{A} \tag{6}$$

where $A' = \partial_x A$. This equation clearly shows that the combined limits $A \to 0$ while $\partial_x A \neq 0$ will tend to either choke the flow $\partial_t \rho \to \infty$ or allow supersonic flow $\partial_x v \to \infty$. Unfortunately, the presence of the additional velocity term $v$ on the RHS means that this equation is most easily satisfied with $v = 0$ ensuring that choking occurs. We will later show that the squeezed systems considered in this paper, duplicate solid-fuel rockets in that mass and momentum injection, reinforce each other to drive ever faster and hotter expelled flows, which suggests that choked flows will not be a necessary feature of squeezed systems.

Mathematically, squeezing an arbitrary fluid introduces regular singular points into the governing equations, which can force singular solutions as shown by the zeroth order Bessel's equation for $\rho(y)$:

$$y(\rho'' + \rho) = -\rho' \tag{7}$$

The finite Bessel function of the first kind $\rho(y) = J_0(y)$ has $J_0'(0) = 0$ trivially satisfying the equation at the origin. In contrast, the unbounded Bessel function of the second kind $\rho(y) = Y_0(y)$ has gradient $Y_0'(0) \neq 0$ and $y \to 0$ forces $[Y_0''(0) + Y_0(0)] \to -\infty$ and $Y_0'(0) \to \infty$.

## III. Fluid Dynamics in Squeezed Cavities

Most fluid dynamical flow problems are solved in regions defined by stationary boundaries. In contrast, we consider a region with dynamic boundaries chosen to change the nature of the solutions of the system of fluid equations. The boundary dynamics are described by their own boundary equations, which are additional to the usual fluid equations. Adding further equations to a given system of equations will usually change the nature of the solution space.

Consider the fluid in a region contracting because of external applied forces as shown in Fig. 1. Here a board of length $L$ and width $W$ are descending at velocity $w$ toward a surface. The enclosed fluid is moving with velocity $(v_x, v_y)$ and is expected to be ejected from between the boards into the outside uncompressed region as the internal pressure builds up. (We exploit symmetry to ignore the $z$ direction.) We model the separation distance as $d(t) = d_0 f(t)$, with time-dependent function chosen so that $f(0) = 1$ and $w = d_0 \dot{f}$.

This system is entirely described by the usual Euler equations together with dynamical boundary conditions specifying that the fluid velocity is constrained to have $v_y = w$ along the top and bottom surfaces of the descending board and to have $v_x = 0$ on the rightmost vertical edge of the board. (Here we consider an inviscid fluid.) An entirely identical description of this squeezed physical system can be obtained by making a time-dependent coordinate transformation

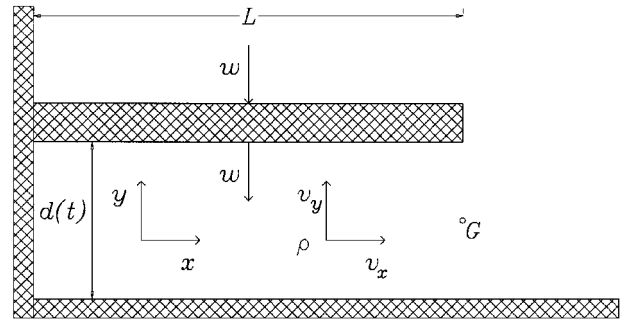


**Fig. 1 Squeezed geometry.**

$$x = x, \qquad y = f(t)\chi + g(t), \qquad t = t \tag{8}$$

designed to mathematically render the moving board stationary. This result is achieved by choosing $f(t)$ and $g(t)$ so that as the board in real space changes its $y$ position the functions $f$ and $g$ are varied so as to leave the $\chi$ position of the board constant in computational space. Standard change of coordinate methods[23] or consultation of the helpful Ref. 24 then give the computational space fluid equations as

$$\partial_t U + \partial_x F + \partial_\chi G = 0$$

$$U = \begin{bmatrix} f\rho \\ f\rho v_x \\ f\rho v_y \end{bmatrix}, \qquad F = \begin{bmatrix} f\rho v_x \\ f\left(\rho v_x^2 + \rho^\gamma/\gamma\right) \\ f\rho v_x v_y \end{bmatrix} \tag{9}$$

$$G = \begin{bmatrix} f\rho v_\chi \\ f\rho v_x v_\chi \\ f\rho v_y v_\chi + \rho^\gamma/\gamma \end{bmatrix}$$

Here, we mix terms $v_y$ and $v_\chi = (v_y - \dot{f}\chi - \dot{g})/f$ to maximally simplify the equations and show the mass continuity (top line) and momentum conservation equations in the $x$ and $y$ directions with velocities $v_x$ and $v_y$, respectively. The adiabatic limit is realized by relating fluid pressure $p$ to fluid density $\rho$ as $p = \rho^\gamma$, where $\gamma = 1.4$ is the usual ratio of specific heats. All variables are dimensionless with dimensioned (primed) variables being given by $x' = xL$, $v' = va_0$, $p' = pp_0$, $\rho' = \rho\rho_0$, and $t' = tL/a_0$ with $L$ being some convenient length parameter and $a_0^2 = \gamma p_0/\rho_0$ is the local speed of sound in ambient pressure and density conditions of $p_0$ and $\rho_0$. With these choices a unit velocity equates to the speed of sound in the fluid.

In real space the squeezing of the boards compresses the inside air to expel a jet of air, whereas in computational space the board is stationary and squeezing forces are converted into mass and momentum injection sources. These inject matter everywhere into the space between the boards to raise the density and to expel the observed jet of air. We thus expect that the squeezed system is equivalent to a mass-injection solid-fuel rocket.[1,2] That this expectation is reasonable can be shown by considering the case of linear squeezing $f(t) = 1 - t/T$, $\dot{f} = -1/T$, $g = 0$ where $T = d_0/w$ is the closure time of the cavity. Further, when the cavity length is much greater than the height $L \gg d(t)$, then sound waves can rapidly traverse the height of the cavity many times to smooth vertical velocities so that $v_\chi = 0$, $v_y = \dot{f}y$, and $\partial_\chi \rho = 0$, which reduces the Euler equations to

$$\partial_t \begin{bmatrix} f\rho \\ f\rho v_x \end{bmatrix} + \partial_x \begin{bmatrix} f\rho v_x \\ f\left(\rho v_x^2 + \rho^\gamma/\gamma\right) \end{bmatrix} = 0 \tag{10}$$

or in injection form

$$\partial_t \begin{bmatrix} \rho \\ \rho v_x \end{bmatrix} + \partial_x \begin{bmatrix} \rho v_x \\ \rho v_x^2 + \rho^\gamma/\gamma \end{bmatrix} = -\frac{\dot{f}}{f} \begin{bmatrix} \rho \\ \rho v_x \end{bmatrix} \tag{11}$$

This clearly shows a one-dimensional system with mass and momentum injection terms of $-\dot{f}\rho/f$ and $-\dot{f}\rho v_x/f$, respectively. Thus, a squeezed system is equivalent to a fuel-injected rocket, but as $f \to 0$ with an ever-increasing mass of fuel injected with an ever increasing momentum. This system is not expected to undergo choking. These equations also demonstrate that we expect large expulsion velocities in either the case of large wall velocities, $\dot{f} \approx 1$ in dimensionless units, or when $f \to 0$ to access the singularity.

## IV. Analytic Solutions to Squeezed Systems

In this section we provide approximate analytic solutions for the fluid flow in squeezed systems. A physical understanding of the squeezed system of Fig. 1 is readily had by considering a constant density approximation that allows equating the loss of internal volume $\delta V = -LWw\delta t$ with the gain in volume of the expelled jet $\delta V = Wd(t)v(L,t)\delta t$ giving

$$v(L,t) = -wL/d(t) = -\dot{f}L/f \tag{12}$$

Simple experiments confirm the importance of the spatial amplification factor $L$: clap your hands with fingers together ($L \approx 3$ cm) and with fingers apart ($L' = L/4$) noting the different sounds.

A first solution of interest is obtained for the one-dimensional fuel-injected rocket, Eq. (10), when we consider a squeezed cavity with both ends closed—a piston—obtained by setting all $x$ gradients and $v_x$ equal to zero, which reduces Eq. (10) to $\partial_t(f\rho) = 0$ with nondimensional solution

$$\rho(t) = 1/f \tag{13}$$

showing the expected singularity in density as $f \to 0$ for this piston system.

A second solution applies to an open-ended cavity with nonzero $x$ gradients and velocities $v_x \neq 0$. We still consider expulsion velocities small enough to satisfy $v_x^2 = 0$. If we then assume approximately constant density $\rho = 1$, then Eq. (10) is satisfied by

$$v_x(x,t) = -\dot{f}x/f \tag{14}$$

which extends the previous heuristic solution of Eq. (12). This solution is strictly valid only while $v_x < 0.3$, where free-flowing air remains approximately uncompressed, but this is expected to be satisfied for initial stages of squeezing.

These approximate solutions can be used to gain some insight into the structure of the expelled air jet. In time $\delta t$, a mass $\delta m = \rho LWd_0\dot{f}\delta t$ is expelled at velocity $v_x(L,t)$ given by Eq. (14) and with kinetic energy $\delta E = \frac{1}{2}\delta m v_x^2$, and this integrates to give total mass expulsion to time $t$ of

$$m(t) = m_0(1-f) \tag{15}$$

and total kinetic energy of the expelled jet of

$$E(t) = -E_p T^2 \int_0^t \mathrm{d}t\left(\frac{\dot{f}^3}{f^2}\right) \tag{16}$$

where $m_0 = \rho LWd_0$ is the initial fluid mass and $E_p = \frac{1}{2}m_0(L/T)^2$ is the kinetic energy of a mass $m_0$ moving over distance $L$ in closure time $T$. For the linear squeezing case with loss of volume given by $\delta V/V = t/T = 1-f$, this gives

$$E = E_p(t/Tf) \tag{17}$$

This last relationship shows the kinetic energy of the expelled jet showing a singularity as $f \to 0$.

The velocity solution of Eq. (14) can also be used to suggest the evolution of spatial density concentrations along the length of the expelled jet that might source shock waves formation. Consider a jet with expulsion velocity given by Eq. (14) expelled into an external environment of low density so we can ignore external frictional braking. The position at closure time $T$ of a particle expelled at the earlier time $t$ is then

$$X(t,T) = L + v(L,t)(T-t) \tag{18}$$

For linear squeezing we have $f(t) = (1-t/T)$ giving $X(t,T) = 2L$ for all of the expelled particles in the air jet implying an approximate density distribution of

$$\rho(x,T) \propto \delta[x-2L] \tag{19}$$

Such density concentrations, if large enough, can source the formation of shock fronts within the jet. We note that this elementary treatment ignores vortex dynamics in the expelled jet and turbulence.

## V. Numerical Simulations

Squeezed cavities are analytically intractable and necessitate a resort to computational fluid dynamics (CFD). CFD approaches can be used to gain insight into the dynamics of squeezed systems but are severely limited as the simulation of a singularity requires an ever finer computational mesh, and the increasing computational load will eventually overwhelm the capacity of any computer. Further, it is not entirely clear that CFD approaches will, even in principle, be able to distinguish between common divergences caused by instabilities in the code and singularities present in the solution. This section provides an initial assessment of the ability of the simplest of CFD approaches to model squeezed systems. We use MacCormack's technique, which employs an explicit finite element method that is second-order accurate in space and time.[25,26]

Consider a cavity of length $L = 30$ cm and height and width $d_0 = W = 5$ cm. The cavity undergoes a linear compression $d(t) = d_0 f(t)$ with $f = 1 - t/T$, giving closure velocity $w = d_0\dot{f} = -d_0/T = -10$ m/s and $T = -d_0/w = 5$ ms.

A qualitative understanding of the simulations can be obtained as follows. The closure of the cavity will raise the internal density and cause the cavity to begin to evacuate as a rarefaction wave propagates from the open end into the cavity. This wave front will move at the local speed of sound, so that the wave will take about $L/a_0 \approx 1$ ms to traverse the full length of the cavity. During this time, sound waves can cross the height of the cavity many times to equilibrate the density in the vertical direction. Also, before the wave front arrives fluid gradients in the $x$ direction are necessarily zero, and so the piston solution of Eq. (13) is applicable. Qualitatively then, we expect our simulations to show a rarefaction wave propagating from the open end of the cavity into a region showing a density increase proportional to $1/(1-t/T)$ with a singularity as $t \to T$. The expulsion velocity gradients are driven by the density gradients between the inside of the cavity and the outside with $\rho = 1$ suggesting expulsion velocities going as $v_x \propto \rho(t) - 1 \propto 1/(1-t/T)$ again showing a singularity as $t \to T$. These qualitative discussions are borne out in the simulations.

The CFD numerical simulation is shown in Fig. 2, which shows the squeezing board as being stationary in computation space while dropping in physical space to cause a 2% compression in graph Fig. 2a and a 10% compression in graph Fig. 2b. The left and bottom walls are not shown for clarity. We note that three separate coordinate transformations are used in these figures to represent those parts of the physical space that are being squeezed, being expanded, or merely being translated. This means that the $y$ axis contains three vertical time-dependent scales as shown.

In graph Fig. 2a we see that a compression wave of higher density is propagating in the $-y$ direction away from the moving edge of the board. This region of higher density then begins to exhaust from the cavity as a rarefaction wave begins to propagate at the local speed of sound into the region of higher density. The difference in horizontal and vertical scales makes the rarefaction wave appear to move a smaller distance than the compression wave. In graph Fig. 2b we see that the compression has approximately equilibrated the density across the cavity, and with 10% squeezing ($f = 0.9$) the density has increased as predicted by Eq. (13) with $\rho = 1/f = 1.11$ atmospheres. This result gives us some confidence in the accuracy of the numerical simulations. The rarefaction wave has propagated about half the length of the cavity at this time. Once the air begins to evacuate, the piston solution is no longer valid, and we must consider the velocity solution of Eq. (14) with its linear dependence on position $x$. The validity of this linear solution is well demonstrated in Fig. 3 at the time of 10% squeezing giving confidence in the numerical simulations. The rarefaction wave has traveled about

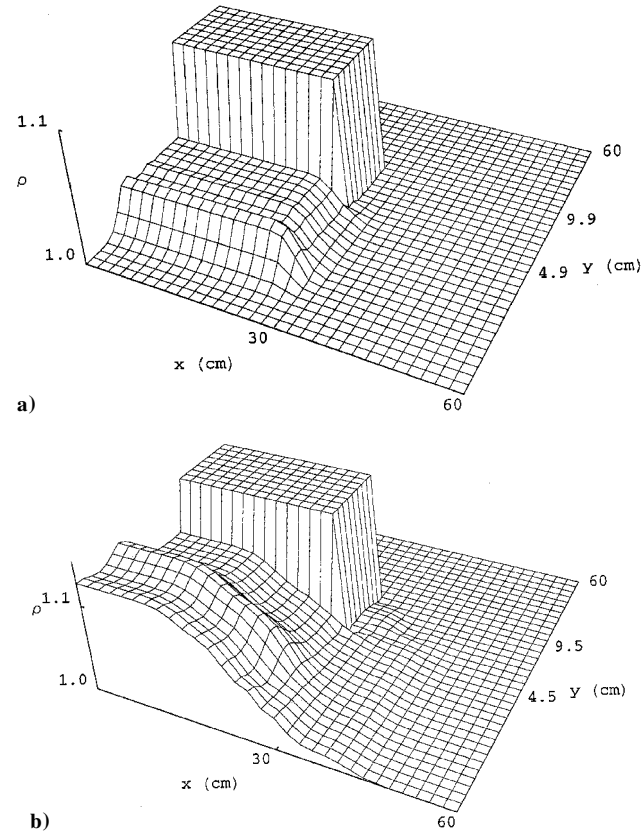


**Fig. 2 Density profile of the air contained within the squeezed cavity (with left and bottom walls not shown) at times representing a) 2% squeezing at $t = 0.1$ ms and b) 10% squeezing at $t = 0.5$ ms. The density is given in dimensionless units with the maximum pressure observed in b) with 10% squeezing ($f = 0.9$) as predicted by Eq. (13) with $\rho = 1/f = 1.11$ atmospheres. (Note the changing scales along the $y$ axis.)**

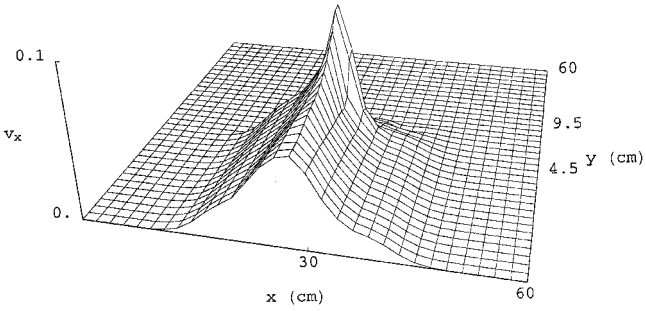


**Fig. 3 Linear dependence of expulsion velocity on position $x$ as predicted in the analytic solution of Eq. (14) is shown in dimensionless units at time $t = 0.5$ ms. At this time we have 10% squeezing with about half the cavity evacuating. (Note the changing scales along the $y$ axis.)**

half the length of the cavity, and the evacuating air clearly shows the expected linear increase of velocity with position. (Note that the air accelerates around the sharp corner of the board giving higher velocities.)

A grid-dependence test was performed to assess the quality of the simulations and compared flow parameters at the point labelled G in Fig. 1 located exactly half way between the descending board and the bottom surface (Table 1). Here we see that a doubling of the grid density causes only small changes in calculated fluid parameters of order $8 \times 10^{-3}$ for 10 and 20% squeezing and increasing to $4 \times 10^{-2}$ for 30% squeezing. The simulations demonstrate grid independence for small squeezing, so that we restrict all simulations to a maximum of 10% squeezing and employ a grid of $61 \times 61$ points (not all lines are drawn in the figures). The causes of the increasing error for large values of the squeezing include the sharp corners of the falling board, the absence of artificial viscosity because of difficulties caused by the complex time-dependent coordinate systems, and

**Table 1 Grid-independence test comparing fluid parameters for grid sizes $61 \times 61$ and $121 \times 121$[a]**

| Time | % Squeezing | $\rho$ | $\Delta\rho$ | $v_x$ | $\Delta v_x$ |
|---|---|---|---|---|---|
| | | *Grid* $61 \times 61$ | | | |
| 0.567 | 10 | 1.05467 | —— | 0.060118 | —— |
| 1.134 | 20 | 1.06879 | —— | 0.165234 | —— |
| 1.701 | 30 | 1.06371 | —— | 0.272322 | —— |
| | | *Grid* $121 \times 121$ | | | |
| 0.567 | 10 | 1.04627 | 0.0084 | 0.066700 | 0.0066 |
| 1.134 | 20 | 1.05956 | 0.0092 | 0.174244 | 0.0090 |
| 1.701 | 30 | 1.01985 | 0.044 | 0.334438 | 0.062 |

[a]We show elapsed time and percentage squeezing $= [1 - f(t)]$ with density $\rho$, expulsion velocity $v_x$, and simulation differences.

reflected waves caused by the small size of the simulation area. (We later discuss the difficulties of satisfying the Courant stability and accuracy conditions.)

The numerical observations of the rarefaction wave can be quantified as follows. The rarefaction wave necessarily moves at the local speed of sound, which is determined by the local density obtained from the heuristic piston solution of Eq. (13). This gives the local speed of sound at position $(x, t)$ before the arrival of the rarefaction wave as

$$a(x,t) = -\rho^{(\gamma-1)/2} = -(1 - t/T)^{-(\gamma-1)/2} \tag{20}$$

The rarefaction wave starts at position $x = 1$ and propagates to the left with the rarefaction wave front located at

$$x_r(t) = L - [2a_0 T/(3-\gamma)]\left[1 - (1 - t/T)^{(3-\gamma)/2}\right] \tag{21}$$

in dimensioned units. This immediately gives the maximum distance that a rarefaction wave can travel by the closure time $T$ as

$$x_{\max}(T) = L - x_r(T) = 2a_0 T/(3-\gamma) \tag{22}$$

All fluid to the left of this moving wave has zero horizontal velocity and has density well-described by the piston Eq. (13). The preceding condition also serves as a guide to experimental design as maximum expulsion velocities are obtained by maximizing the density gradients that occur when the rarefaction wave just has time $\tau_t$ to traverse the full length of the cavity $\tau_t \approx L/a_0$ as closure occurs $\tau_c \approx d_0/w$. Relating these two time scales $\tau_t$ and $\tau_c$ gives experimental design guidelines:

$$\begin{aligned} wL/d_0 &\ll 2a_0/(3-\gamma) \text{ (low Mach speeds)} \\ &\approx 2a_0/(3-\gamma) \text{ (high Mach speeds)} \\ &\gg 2a_0/(3-\gamma) \text{ (fluid trapped, high Mach speeds)} \end{aligned} \tag{23}$$

The experiment discussed in the next section has $d_0 = 5$ cm, $L = 30$ cm, and $w = 10$ m/s, so that our experimental parameters give $wL/d_0 = 60$ m/s $\ll 2a_0/(3-\gamma) = 425$ m/s and thus has scope for design improvements giving expulsion velocities greater by a factor of at least seven.

The timescale of the preceding simulations has been carefully restricted to ensure that the simulations are stable and accurate and to minimize the effects of reflections from the simulation boundary. In all cases the simulations have demonstrated grid independence (with doubling of grid sizes) and by the successful comparisons with analytic results. At this stage the simulations cannot be extended to show supersonic flow as satisfying the Courant condition is difficult in this squeezed system. The Courant condition for stability in hyperbolic equations requires that the simulation time step is shorter than the minimum time taken by a sound wave to travel across a grid step. In the squeezed system considered here, the vertical grid is shrinking in time by the factor $f(t) \to 0$, whereas the horizontal grid size is unchanging. The Courant condition then maintains stability by forcing the time step to shrink to zero. Unfortunately this decreases the accuracy of the solution as the numerical domains for information influencing a grid point begin to vastly exceed the analytic domains of that point leading to dynamic instabilities with their

characteristic exponentially growing alternating positive and negative errors.[25] We thus expect our numerical simulation to fail at just the point of interest as $f(t) \to 0$, and so we restrict our simulation times appropriately. Squeezed cavities are generally numerically intractable, and we now turn to consider experimental verification of the flow speeds of expelled jets.

## VI. Experiments with Expelled Air Jets

The preceding results are counterintuitive because of their novelty, and so a rough experiment was conducted to assess their reliability.

Two boards of length $L = 30$ cm were hinged together at one end while side walls were used to ensure that expelled air traversed the full length $L$. The boards were slapped together at speeds of about $w = 10$ m/s with the freestream $p_\infty$ and static $p_0$ pressures of the expelled jet being measured by pressure transducers of diameter around 5 mm and of sensitivity about 114.2 mV/psi. (The large size of these transducers causes underestimation of jet velocities in the final stages of closure when the jet is less than 5 mm in height.) The expelled jet lasted only for milliseconds with measurement timescales of interest lasting only some tens of microseconds, which necessitated use of a 40-MHz virtual capture oscilloscope to read the transducer signals.

The pressure readings were converted to a Mach speed using standard subsonic or supersonic formula[2] and are shown in Fig. 4. Also shown here is the theoretical curve for incompressible air expelled from hinged boards:

$$v_x = \frac{L}{2(T-t)a_0} \tag{24}$$

normalized to the speed of sound $a_0 = 340.252$ m/s. This result differs from Eq. (12) by a factor of $\frac{1}{2}$ as hinged boards trace pseudo-triangular arcs of half the area of the previous rectangles. There is excellent agreement between theory and experiment in the regime of validity $v_x < 0.3$.

Maximum measured jet speeds occurred with $p_0 = 1.76 \pm 0.07$ and $p_\infty = 0.74 \pm 0.07$ atmospheres to give a Mach speed of $1.19 \pm 0.07$ and flow speed of $386 \pm 21$ m/s, which is roughly in accordance with the heuristic analysis of Eq. (24) with the expected expulsion velocity in the last 0.5 cm of closure [$d(t) = 0.5$ cm] being $v \approx Lw/[2d(t)] \approx 10 \times 0.3/(2 \times 0.005) \approx 300$ m/s.

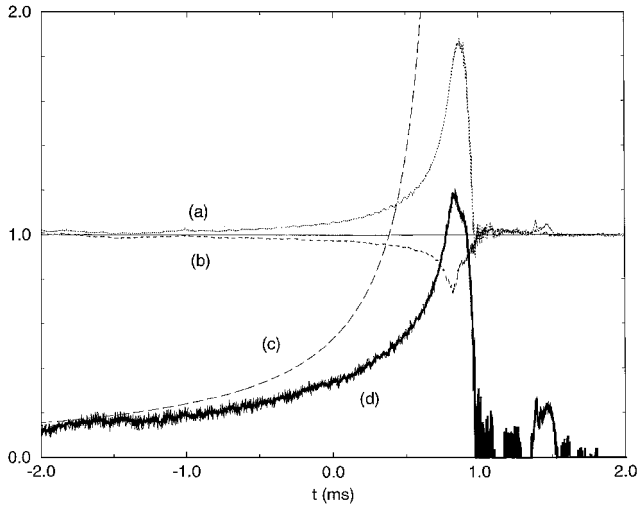


**Fig. 4 Expelled jets from squeezed systems. The trigger time is at $t = 0$ with estimated closure time $T = 0.825$ ms. Curves shown are (a) the stagnation pressure $p_0$ (atm), (b) the freestream pressure $p_\infty$ (atm), (c) the heuristic normalized expulsion velocity for incompressible fluids $v = L/[2(T-t)a_0]$, and (d) the Mach speed of the expelled flow. The measurement errors in the pressure readings (a) and (b) are ± 0.07 atmospheres giving a calculated error for the maximum Mach speed of 1.19 ± 0.07 (curve d). There is excellent agreement between the analytic predictions (c) and experiment in the regime of validity $v_x < 0.3$ in dimensionless units.**

Experimental errors in flow speeds are determined analytically from a combination of the measured calibration curves of each individual pressure transducer together with an estimated error allowance for turbulence and flow disturbance caused by the pressure transducers. Estimates are subsequently justified by examination of the variance of the calculated flow speeds and by comparison to analytic results.

We note that a number of simple design changes can modify the geometry and velocities in this experiment to drive higher escape velocities. These include doubling the length of the cavity $L \to 2L$, doubling the closure velocity $w \to 2w$ by using a longer hammer, and shrinking the initial height of the cavity $d_0 \to d_0/2$. We further expect that more sensitive measurement techniques such as laser Doppler velocimetry might conceivably double observed velocities as the current pressure transducers have diameter around 5 mm and cannot properly measure jets of height 1 mm. The possibility also exists that increasing the internal air pressure by narrowing the escape channel (to borrow from standard shock tunnel technologies) might also increase escape flows by a factor of two. All together, these speculations suggest that it is possible that significant expelled flow velocities might be possible from hand-powered and tabletop squeezed systems. The experiment of this section has served as a proof of concept, and investigation of higher-speed flows will be the subject of later reports.

## VII. Conclusion

We have demonstrated that squeezing an arbitrary fluid system embeds regular singular points into the equations of motion, which can drive solutions to singularities. These singularities can be harnessed in piston systems to access extreme fluid temperatures and densities. We show analytically and experimentally that these same singularities can elegantly drive supersonic expelled flows from squeezed systems. The significance of this demonstration lies in recognizing that squeezing drives many expulsion processes in nature including fissioning fluid drops or evaporating fluid surfaces, astrophysical systems with large crushing gravitational fields, and in unexplained sound emission from squeezed cavities in car tires, among others.

This paper also provides an additional demonstration that dynamic boundary conditions can radically change the solution space of the partial differential equations governing fluid flow. While fluid flows through pipes, around objects or in regions with stationary boundaries offers complex dynamical behaviors, adding time-dependent boundaries vastly enriches the available solution space. In this era of high-powered computers it is no longer necessary to avoid investigating systems with dynamical boundaries. Hopefully this paper will stimulate investigations into a wider range of time-dependent boundary conditions that radically modify solution characteristics.

To address the interesting problem of the interaction between the two boundary layers attached to the squeezing walls as the walls close to zero separation is beyond the scope of this paper. Although it is not at all clear what compressed, sheared, and interacting boundary layers will do, viscous flows lie outside the scope of this project. We further note that squeezed systems cannot easily be characterized by a single Reynolds number usually defined in terms of some typical flow length $L$ as

$$R = \rho v L/\mu \tag{25}$$

with fluid viscosity $\mu$. The interesting dynamics in squeezed systems appears in the final stages of closure when the cavity length $L = 30$ cm is greater than the cavity height $d(t) = 1$ mm by a factor of 300. The Reynolds number determines the characteristics of flow, and it is not clear what happens in squeezed systems that feature time-dependent lengths on both macroscopic and microscopic scales. Squeezed systems are characterized by ill-defined and time dependent Reynolds numbers.

## Acknowledgments

Initial stages of this work were completed at the Yukawa Institute of Theoretical Physics, Kyoto University, Japan, with the support of the Japan Society for the Promotion of Science and the Japanese

Ministry of Education, Science and Culture (Mombusho). The author gratefully acknowledges discussions with Henri Boffin.

## References

[1]Zucrow, M. J., and Hoffman, J. D., *Gas Dynamics*, Wiley, New York, 1976.

[2]Warsi, Z. U. A., *Fluid Dynamics: Theoretical and Computational Approaches*, CRC Press, Boca Raton, FL, 1993.

[3]Glass, I. I., and Sislian, J. P., *Nonstationary Flows and Shock Waves*, Clarendon, Oxford, 1994, pp. 19–35.

[4]Jayaraman, A., "Diamond-Anvil Cell and High-Pressure Physical Investigations," *Reviews of Modern Physics*, Vol. 55, No. 1, 1983, pp. 65–108.

[5]Young, F. Y., *Cavitation*, McGraw–Hill, New York, 1989, pp. 318–350.

[6]Weninger, K. R., Barber, B. P., and Putterman, S. J., "Pulsed Mie Scattering Measurements of the Collapse of a Sonoluminescing Bubble," *Physical Review Letters*, Vol. 78, No. 9, 1997, pp. 1799–1802.

[7]Barber, B. P., Hiller, R. A., Löfstedt, R., Putterman, S. J., and Weninger, K. R., "Defining the Unknowns of Sonoluminescence," *Physics Reports*, Vol. 281, No. 2, 1997, pp. 65–143.

[8]Lohse, D., Brenner, M. P., Dupont, T. F., Hilgenfeldt, S., and Johnston, B., "Sonoluminescing Air Bubbles Rectify Argon," *Physical Review Letters*, Vol. 78, No. 7, 1997, pp. 1359–1362.

[9]Hill, S., Sandhu, P. S., Qualls, J. S., and Brooks, J. S., "Bulk Quantum Hall Effect: Evidence That Surface States Play a Key Role," *Physical Review B*, Vol. 55, No. 8, 1997, pp. R4891–R4894.

[10]Hill, S., Valfells, S., Uji, S., Brooks, J. S., Athas, G. J., Sandhu, P. S., Sarrao, J., Fisk, Z., Goettee, J., Aoki, H., and Terashima, T., "Quantum Limit and Anomalous Field-Induced Insulating Behaviour in $\eta$- $Mo_4$ $O_{11}$," *Physical Review B*, Vol. 55, No. 4, 1997, pp. 2018–2031.

[11]Remington, B. A., Kane, J., Drake, R. P., Glendinning, S. G., Estabrook, K., London, R., Castor, J., Wallace, R. J., Arnett, D., Liang, E., McCray, R., Rubenchik, A., and Fryxell, B., "Supernovae Hydrodynamic Experiments on the Nova Laser," *Physics of Plasmas*, Vol. 4, No. 5, 1997, pp. 1994–2003.

[12]Pelz, R. B., and Gulak, Y., "Evidence of Real-Time Singularity in Hydrodynamics from Time Series Analysis," *Physical Review Letters*, Vol. 79, No. 25, 1997, pp. 4998–5001.

[13]Shi, X. D., Brenner, M. P., and Nagel, S. R., "A Cascade of Structure in a Drop Falling from a Faucet," *Science*, Vol. 265, July 1994, pp. 219–222.

[14]Kadanoff, L. P., "Singularities and Blowups," *Physics Today*, Vol. 50, No. 9, 1997, pp. 11, 12.

[15]Goldstein, R. E., Pesci, A. I., and Shelley, M. J., "Topology Transitions and Singularities in Viscous Flows," *Physical Review Letters*, Vol. 70, No. 20, 1993, pp. 3043–3046.

[16]Mallove, E. F., and Matloff, G. L., *The Starflight Handbook: A Pioneer's Guide to Interstellar Travel*, Wiley, New York, 1989, p. 147.

[17]Fujii, K., "Unified Zonal Method Based on the Fortified Solution Algorithm," *Journal of Computational Physiscs*, Vol. 118, No. 1, 1995, pp. 92–108.

[18]Fujii, K., and Ogawa, T., "Aerodynamics of High Speed Trains Passing by Each Other," *Computers and Fluids*, Vol. 24, No. 8, 1995, pp. 897–908.

[19]Gagen, M. J.,"Expelled Jets from Squeezed Fluid Singularities in Astrophysics" (in preparation).

[20]Gagen, M. J., "Novel Accoustic Sources in Squeezed Cavities in Car Tires," *Journal of the Acoustical Society of America* (to be published).

[21]Halliday, D., and Resnick, R., *Physics*, Wiley, New York, 1960, pp. 472–476.

[22]Kreyszig, E., *Advanced Engineering Mathematics*, Wiley, New York, 1983, pp. 506–519.

[23]Weinberg, S., *Gravitation and Cosmology: Principles and Applications of the General Theory of Relativity*, Wiley, New York, 1972, pp. 47–53.

[24]Hoffmann, K. A., and Chiang, S. T., *Computational Fluid Dynamics for Engineers*, Engineering Education System, Wichita, KS, 1993, pp. 21–31.

[25]Anderson, J. D., *Computational Fluid Dynamics: The Basics with Applications*, McGraw–Hill, New York, 1995, pp. 222–225.

[26]MacCormack, R. W., "The Effect of Viscosity in Hyper-Velocity Impact Cratering," AIAA Paper 69-354, May 1969.

M. Sichel
*Associate Editor*